The Influence of Australian Monsoon Winds on Simultaneous Occurrence of Mountain Waves in Central Java and East Java

Rahmat Alpentido*[1] and Aries Kristianto[2]

[1]*Sultan Muhammad Salahuddin Meteorological Station, Agency of Meteorology Climatology and Geophysics, Bima 84173*
[2]*Department of Meteorology, School of Meteorology Climatology and Geophysics, Tangerang Selatan 15221*

Abstract: Mountain waves are a phenomenon that had occurred due to the interaction of laminar flow in the atmosphere with the contours of the mountains. These waves had been characterized by the presence of lenticular clouds that had formed at the mountain peaks. On the 5th of November 2020, lenticular clouds had formed simultaneously in East and Central Java. During the same period, Australian Monsoon was still active in Java region. Based on these two phenomena, this research had investigated the influence of the Australian Monsoon on the process of mountain wave formation in Central Java and East Java using FNL data. The processing had been carried out using WRF-ARW with resolutions of 9, 3, and 1 km. The results had shown the presence of easterly winds that had affected the atmospheric stability of the Central Java and East Java regions, characterized by the formation of laminar flow, with the formation of laminar flow occurring first in the East Java region. The model output results for potential temperature parameters and visualizations had shown stable atmospheric conditions from the 4th to the 6th of November. The parameter of vertical wind speed had indicated the presence of mountain wave fluctuations in all regions.

Keywords: Mountain Wave; Australian Monsoon; WRF-ARW

*Corresponding author: alpentidosimbolon@gmail.com

http://dx.doi.org/10.12962/j24604682.v20i2.18883
2460-4682

I. INTRODUCTION

Monsoons are wind patterns that form seasonally. It's formed due to the difference in heat received between the land and the ocean [1]. There are two types of monsoon that pass through Indonesia [2]. The monsoons are the Asian Monsoon (west) and the Australian Monsoon (southeast). Monsoon winds can affect local wind conditions. Local wind is the part that affects meso-scale circulation [3]. The Java region, specifically, is influenced by the Australian Monsoon flow which determines the local wind cycle [4]. This circulation can be viewed through the direction of laminar airflow over the ground at the 850 mb layer [5].

Laminar flow is the flow of particles that will sequentially form a straight line without turbulence [6]. Laminar flow is the main factor in the formation of lenticular clouds. Lenticular clouds can form in the presence of mountain waves [7]. These waves are created when steady-state winds hit a topographical obstruction (mountains) and form turbulence when they reach the other side of the mountain [8]. This turbulence is dangerous for aviation and sometimes difficult to predict [3].

Mountain waves occur when the atmosphere is in a stable state. This atmospheric stability can be studied in two ways. The first way is by reviewing the buoyancy frequency using the potential temperature parameter () against height (z), which is called static stability [9]. The second way is to review the frequency of buoyancy and wind shear against turbulence, which is called dynamic stability and is represented by the Richardson Number [10]. In addition, the flow velocity against the speed of gravity can also be used to see the influence of the atmosphere on the formation of mountain waves, or commonly called the Froude Number [11 - 13].

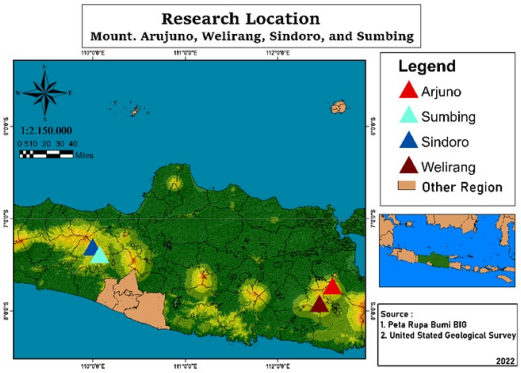

FIG. 1: Research location.

On 5 November 2020, cap clouds (lenticular) formed simultaneously in 7 mountains in the Central Java and East Java Regions [14]. BMKG informed that there was a southeast wind flow in the same period, the first ten-day period of November 2020. This wind flow from the southeast is active until the third ten-day period in November [15]. Based on this phenomenon, a study will be conducted on the influence of the

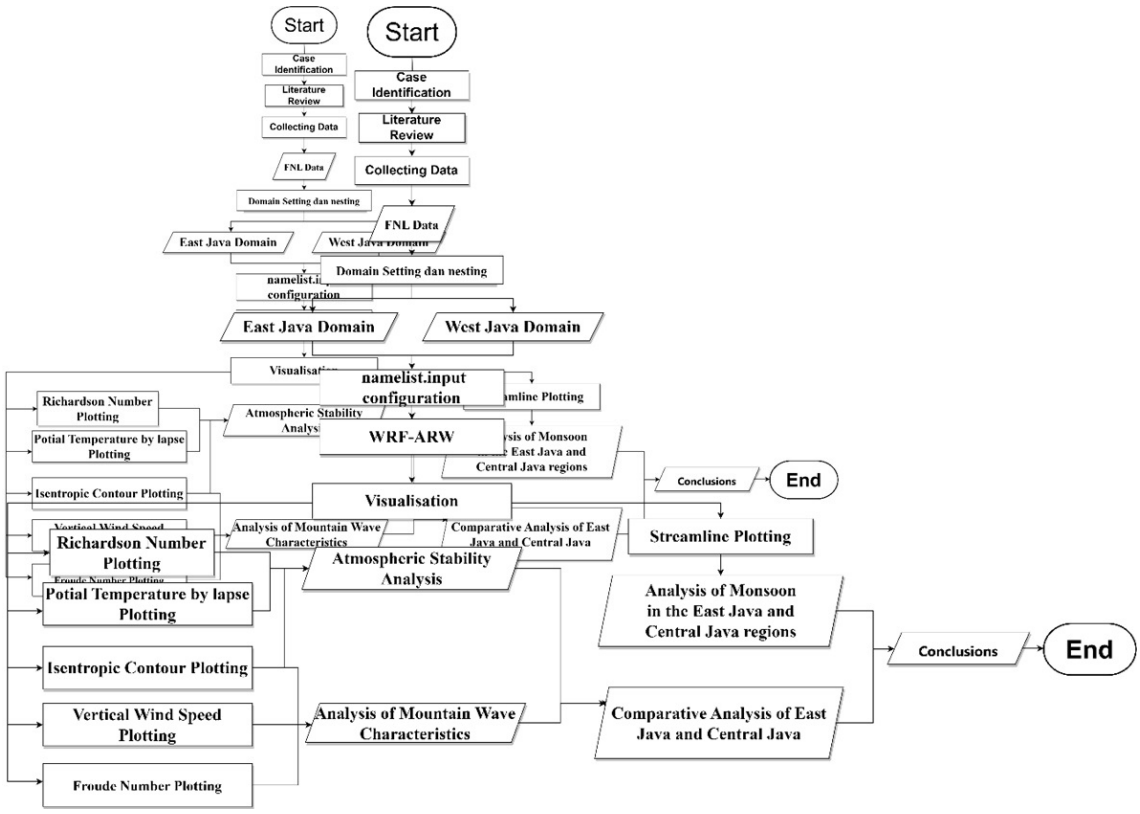

FIG. 2: The research flowchart.

Australian Monsoon on the formation of mountain waves in Central and East Java.

II. METHOD

The phenomenon is studied by visualize the wind direction and speed during the Australian Monsoon and the occurrence of mountain waves at 4 mountain locations. Atmospheric stability parameters (static stability and Richardson Number) and Froude Number will also be used as a comparison when mountain waves occur.

The calculation of Richardson Number [10] is following:

$$Ri = \frac{|g|.\Delta\theta v.\Delta z}{Tv.[(\Delta U)^2 + (\Delta V)^2]} \quad (1)$$

where, *Ri* = Richardson Number; $\Delta\theta v$ = Potential temperature differences (K); g = Gravitational acceleration constant (9.8 m s^{-2}); ΔV = North-south wind speed differences (m s^{-1}); *Tv* = Absolute temperature (K); ΔU = East-west wind speed differences (m s^{-1}); Δz = Height difference (m)

The calculation of Froude Number [10] is Eq. (2).

$$Fr = \frac{U}{Nh_\circ} \quad (2)$$

where, *Fr* = Froude Number; U = surface wind speed while passing through the mountain (m/s); N = Brunt-Vaisala frequency (s^{-1}); $h_\circ$ = height of mountain peaks (m).

The research was conducted at Central Java and East Java. The Central Java region was conducted on Mount Sumbing (7°23'5" N and 110°4'20" E) and Mount Sindoro (7°18'8" N and 109°59'45" E). The two mountains are 12.45 km apart with elevations of 3.371 km and 3.136 km respectively. The East Java region was conducted on Mount Arjuno (7°43'30" N-S and 112°35'21" E) and Mount Welirang (7°54'59" N-S and 112°27' E). The two mountains are 26.29 km apart with an elevation of 3.339 km. The location of the four mountains is shown in Fig. 1.

This research was run for three days. On 4 November 2020 (before the event), 5 November 2020 (during the event), and 6 November 2020 (after the event). Data processing was carried out with the following tools:

1. Weather Research & Forecasting-Advanced Research (WRF-ARW) version 4.1.2
   A modelling application for open-source numerical simulation and prediction of the atmosphere [16]. This latest version of WRF will be used in processing the FNL data. The mountain wave simulation display and its parameters use the Tropical Physics Suite parameterization which is considered to have a high level of validity. [13].

2. Grid Analysis and Display System (GrADS) Version 2.2.1
   GrADS is an earth science data processing application with 4 conventional dimensions (latitude, longi-

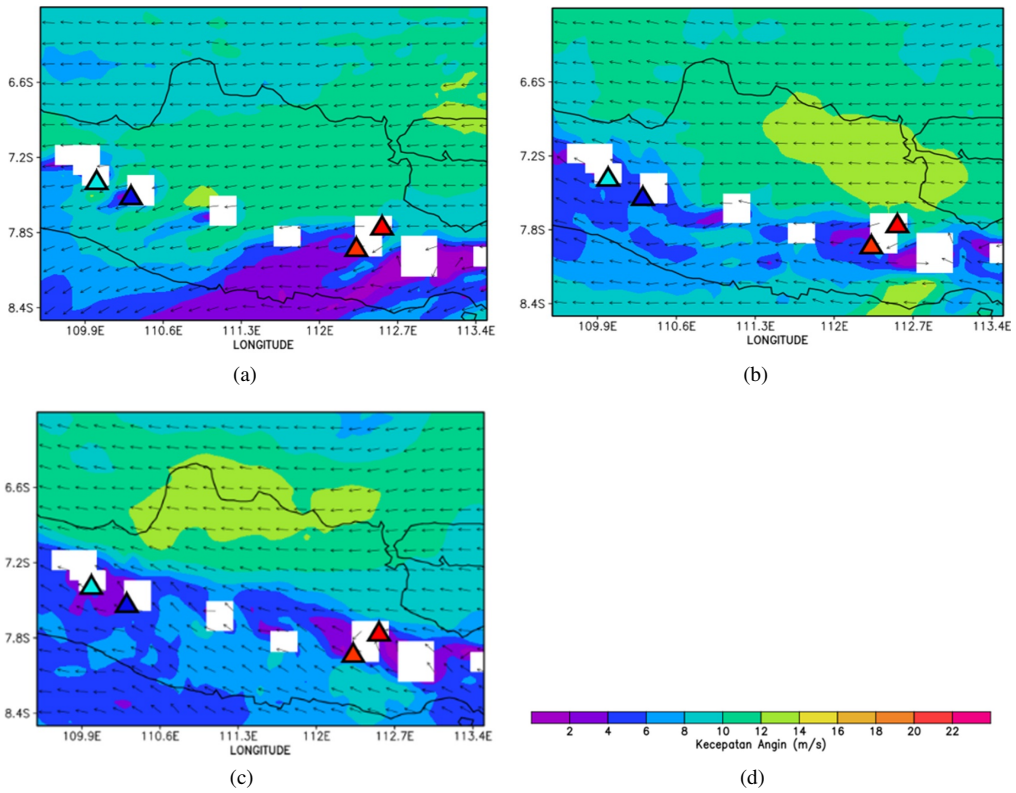

FIG. 3: 850 mb layer wind direction and speed (m/s) at 00 UTC (a) 4 November (b) 5 November and (c) 6 November .

tude, vertical height, and time) and 1 optional dimension Kinter [17]. This latest version of GrADS will be used in the process of visualising the output data from the WRF-ARW model into several parameters.

3. Spreadsheet (Number Processing Application)
   Spreadsheet is an instinctive cell-based application that is structured and simple [18]. This application will be used in the numerical data processing process of visualisation results from GrADS to analyse the comparison of each parameter at different times and locations.

The model output data is processed into the following:

1. The 9 km resolution data was visualised to determine the wind direction and speed in East Java and Central Java.

2. The 1 km resolution data was processed for potential temperature and Richardson Number parameters to determine the dynamic stability of the atmosphere, Froude Number parameters for mountain wave fluctuations, and vertical velocity parameters for mountain wave visualisation. The research flow can be seen in Fig 2.

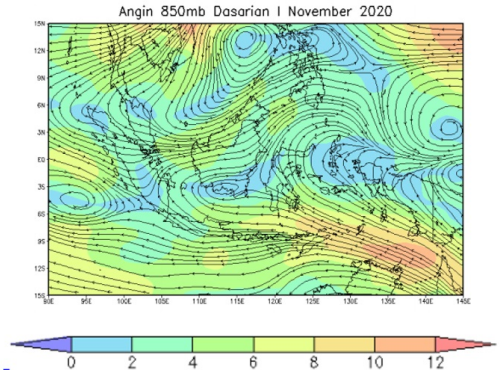

FIG. 4: Wind direction and speed (m/s) of the 850 mb layer in the first ten-day period of November 2020. (Source: BMKG, 2020).

III. RESULT AND DISCUSSION

A. Australian Monsoon

Analysis of monsoon conditions was undertaken in the 850 mb layer. During the case study period (4 to 6 November 2020) the wind direction in the 850 mb layer varied from northeast to southeast (Fig. 3). The triangular symbols in Fig. 3 indicate the mountain locations with light blue for Sindoro, dark blue for Sumbing, red for Arjuno and orange for Weli-

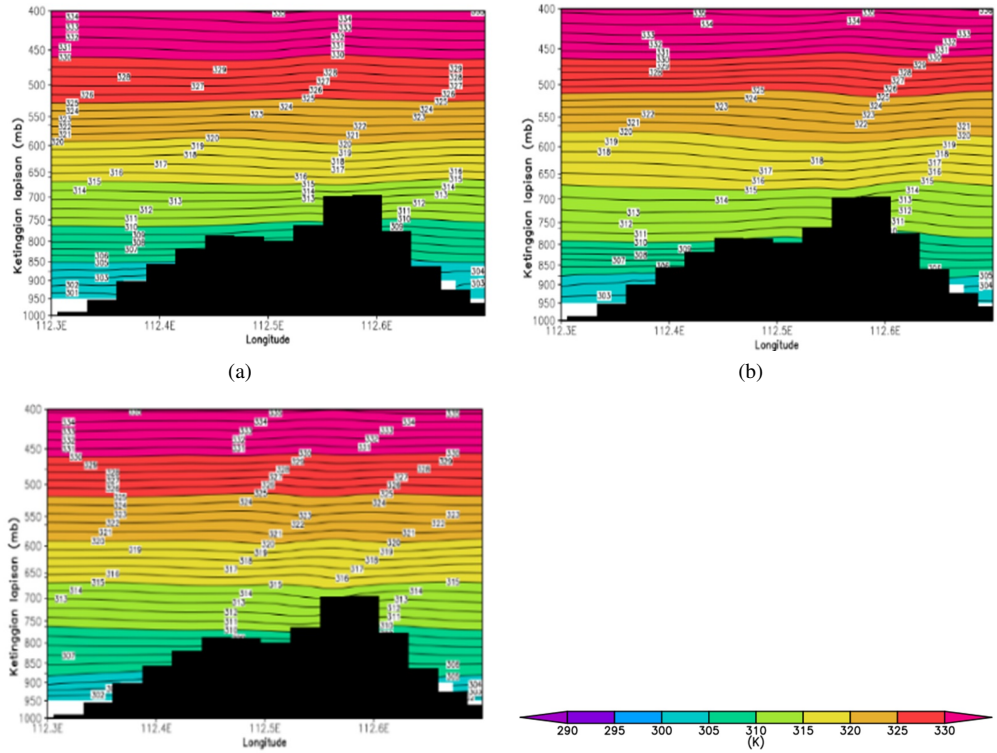

(a) (b)

(c) (d)

FIG. 5: Potential temperature (K) 00 UTC at Mount Arjuno 4 November (b) 5 November dan (c) 6 November.

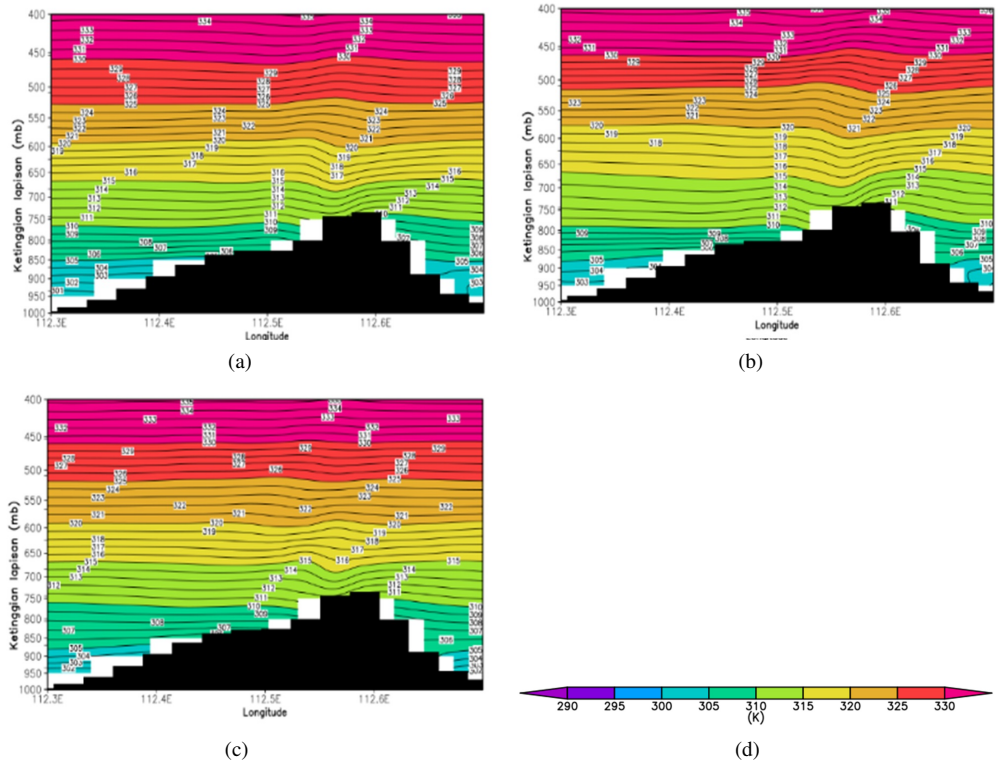

(a) (b)

(c) (d)

FIG. 6: Potential temperature (K) 00 UTC at Mount Welirang (a) 4 November (b) 5 November dan (c) 6 November.

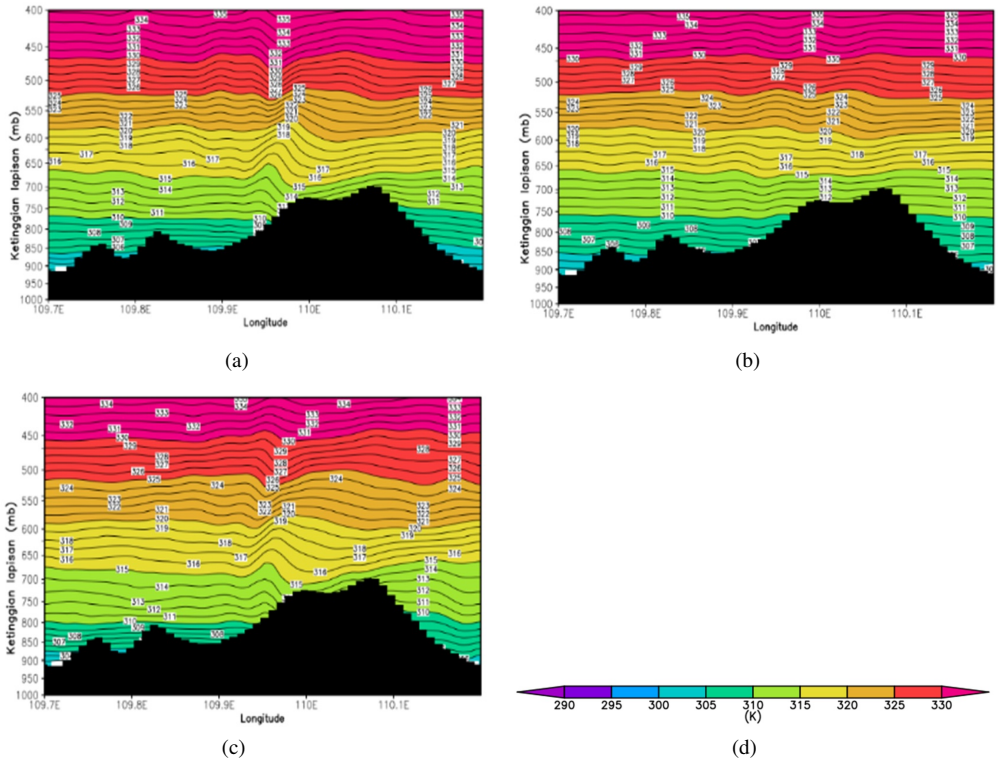

FIG. 7: Potential temperature (K) 00 UTC at Mount Sumbing (a) 4 November (b) 5 November dan (c) 6 November.

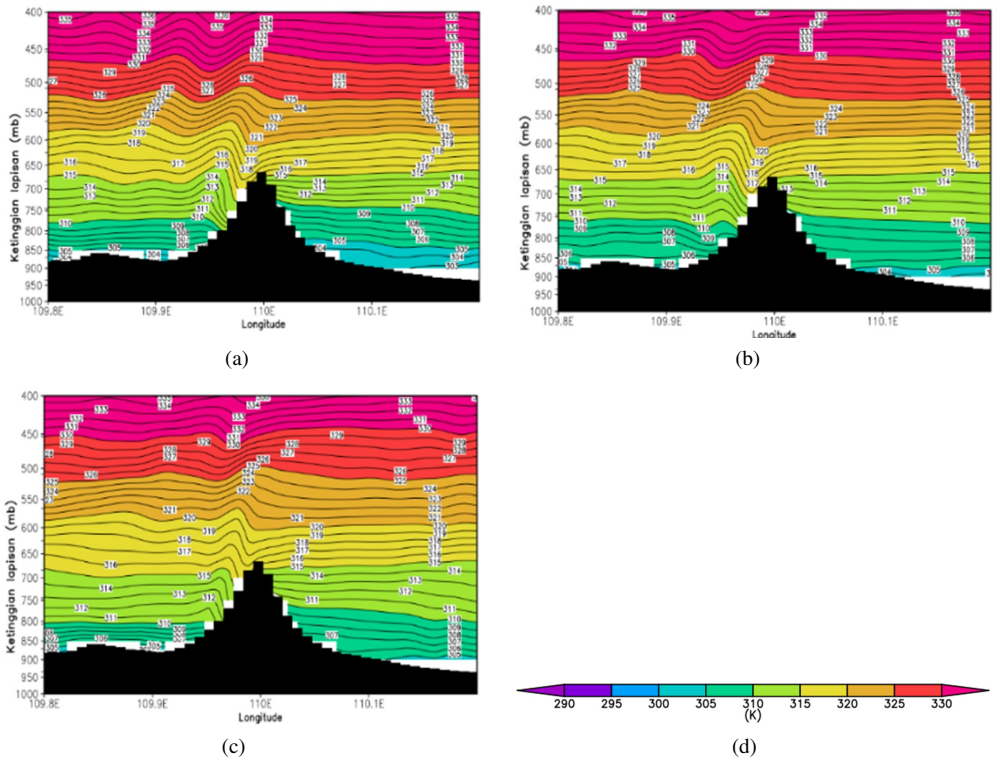

FIG. 8: Potential temperature (K) 00 UTC at Mount Sindoro (a) 4 November (b) 5 November dan (c) 6 November.

TABLE I: Richardson Number at Mount Arjuno and Welirang every hour at 700 mb layer.

HOUR (UTC)	Mount Arjuno			Mount Welirang		
	4 Nov	5 Nov	6 Nov	4 Nov	5 Nov	6 Nov
0	2.85	0.54	0.19	2.02	0.04	0.86
1	6.34	1.89	0.17	0.10	0.03	0.06
2	1.21	0.38	0.09	0.01	0.01	0.01
3	0.80	0.48	0.06	0.01	0.05	0.02
4	0.40	0.49	0.09	0.00	0.03	0.01
5	0.18	0.36	0.28	0.00	0.03	0.04
6	0.10	0.25	0.56	0.00	0.03	3.28
7	0.14	8.48	0.21	0.00	0.02	0.25
8	0.08	1.79	0.09	0.00	0.01	0.01
9	0.03	17.23	0.10	0.00	0.01	0.01
10	0.06	6.37	0.06	0.01	0.10	0.01
11	0.06	2.55	0.06	0.01	0.33	0.06
12	0.05	0.65	0.24	0.03	3.31	0.03
13	0.05	0.20	4.41	0.31	0.05	0.02
14	0.10	0.12	3.49	0.03	0.70	0.03
15	0.17	0.16	5.28	0.55	0.16	0.07
16	0.44	1.12	0.70	2.77	0.11	0.37
17	0.64	3.18	0.86	0.05	0.04	0.10
18	1.80	10.65	2.12	7.27	0.10	0.06
19	1.59	0.21	26.55	0.32	0.21	0.10
20	8.31	0.53	0.24	0.32	1.46	0.80
21	5.41	0.47	0.09	1.08	0.28	0.09
22	7.44	0.12	2.12	0.04	0.48	0.05
23	1.10	0.15	0.59	0.02	4.17	0.10

rang. The white colour in the figure indicates the geographical influence of the mountainous region which results in the wind speed data not being clearly depicted.

Wind speed on 4 November at 00 UTC came from the east to northeast. Wind variations over a 24-hour period were 4-10 m/s in the Central Java region. While in the East Java region the wind speed variation is lower, which is around 2-6 m/s.

On 5 November, the wind direction in Central Java and East Java came from the east. Wind speed in Central Java had a speed variation of 4-8 m/s. Speed variations were more diverse in East Java, ranging from 6-14 m/s. One day after the event, the monsoon wind speed decreased in both study domains. Speed variations in both regions were between 2-8 m/s with a southeast direction.

Overall, the conditions of wind direction and speed passing through Central Java and East Java have the same pattern as the results of the monsoon influence analysis published by BMKG (Fig. 4). This analysis is focused on the first ten-day period of November 2020.

B. Atmospheric Stability

Changes in potential temperature based on altitude can be seen from the distribution of potential temperature around the four mountains. The potential temperature around Mount Arjuno shows an increase in potential temperature based on altitude (Fig. 5). At the top of the mountain, a wavy pattern is

FIG. 9: Time series graph of Froude Number at Mount Arjuno (blue) and Mount Welirang (orange) in the 700 mb layer (a) 4 November (b) 5 November dan (c) 6 November.

formed, which is affected by wind flow and the shape of the mountains.

For the model output at Mount Welirang, there are some white areas in the image indicating the presence of blank data due to the geographical influence of the mountainous region (Fig. 6). But overall, the potential temperature distribution pattern is still clearly depicted in the layer above the surface. The same potential temperature distribution pattern is formed as that of Mount Arjuno.

The distribution of potential temperatures also shows the same trend in the Sumbing Mountain (Fig. 7) and Sindoro Mountain (Fig. 8). The potential temperature range at the top of the mountain ranges from 310 to 315 Kelvin. The value will continue to increase based on altitude up to the 400 mb layer.

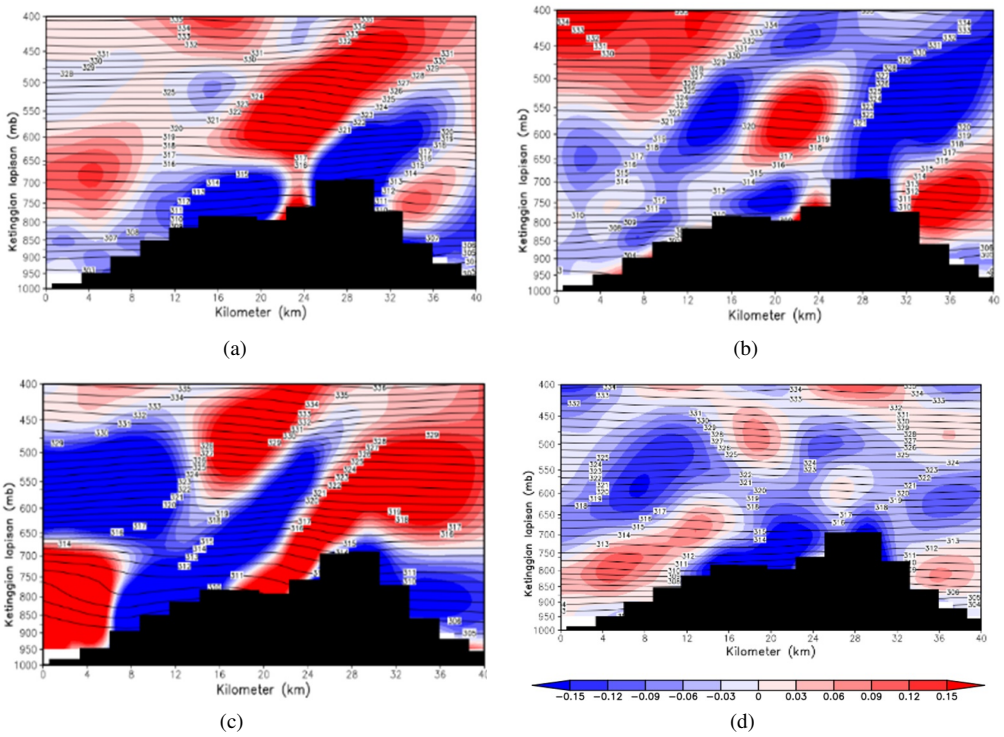

FIG. 10: Vertical velocity (m/s) and isentropic contours at Mount Arjuno (a) 4 November 22 UTC (b) 5 November 02 UTC (c) 5 November 08 UTC (d) 5 November 16 UTC.

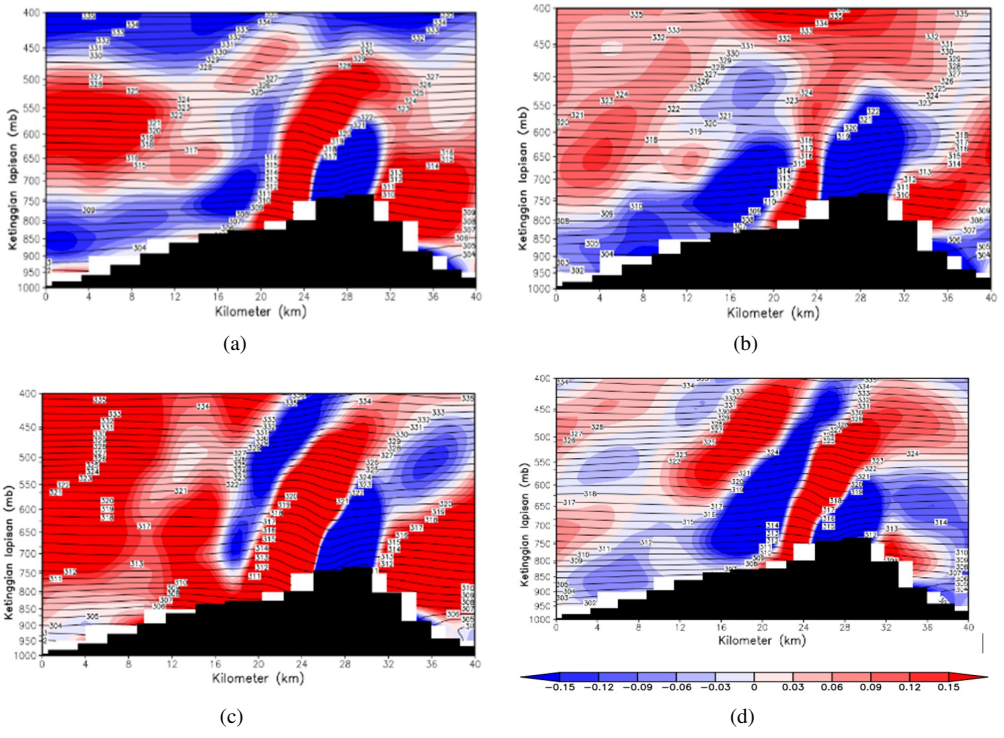

FIG. 11: Vertical velocity (m/s) and isentropic contours at Mount Welirang (a) 4 November 16 UTC (b) 4 November 18 UTC (c) 5 November 01 UTC (d) 5 November 14 UTC.

TABLE II: Richardson Number at Mount Sumbing and Sindoro every hour at 700 mb layer.

HOUR (UTC)	Mount Sumbing 4 Nov	5 Nov	6 Nov	Mount Sindoro 4 Nov	5 Nov	6 Nov
0	0.00	1.32	0.64	5.04	0.00	1.41
1	0.09	0.31	0.04	1.10	2.91	0.68
2	0.26	0.11	0.09	2.19	2.77	2.86
3	0.27	0.12	0.11	1.29	5.39	0.36
4	0.00	2.79	0.14	0.55	0.10	6.19
5	0.35	0.02	0.32	0.27	0.08	0.05
6	0.77	0.02	0.03	0.11	0.02	0.03
7	0.06	0.02	0.04	0.03	0.10	0.05
8	0.14	0.02	0.36	0.02	0.60	0.02
9	0.01	0.00	0.06	70.04	0.20	0.15
10	0.24	0.01	0.97	0.04	0.02	2.42
11	0.12	0.17	0.10	0.10	0.09	0.03
12	0.18	0.05	2.83	0.09	0.12	1.10
13	0.72	0.04	0.04	0.75	0.11	1.44
14	0.20	0.03	0.13	0.27	0.03	19.63
15	0.10	2.50	0.83	0.05	0.22	0.24
16	0.00	0.13	0.96	0.50	0.08	0.46
17	3.95	0.31	1.51	0.16	0.08	0.18
18	0.44	1.87	0.04	1.60	0.13	0.10
19	0.11	23.21	0.44	1.50	0.20	0.15
20	0.15	0.54	0.06	9.07	0.43	0.18
21	0.18	0.33	0.10	1.59	0.42	0.31
22	0.32	0.06	0.08	0.61	1.07	0.00
23	0.41	0.17	0.27	1.43	0.40	0.00

However, a clearer wave pattern is formed on both mountains in Central Java. This indicates the influence of wind on the pattern of potential temperature distribution per layer.

Based on the model output at Mount Sindoro, there are some white areas near the surface, indicating that the model has not been able to describe in detail the conditions occurring in the layer very close to the surface (Fig. 8).

The Richardson Number value describes the dynamic stability conditions. This value is used to assess the timing of the formation of conditions that are supportive of mountain wave formation. These conditions are laminar conditions that are characterised by Richardson Number values that exceed 1.

The distribution of Richardson Number values in the East Java region shows that laminar flow began to form on 4 November at 16 UTC on Mount Welirang. Then the formation of the flow also occurred on Mount Arjuno two hours later, precisely at 18 UTC (Table I). The model output shows a long-lasting laminar flow on Mount Arjuno until 5 November at 01 UTC.

In the Central Java region, there are differences in the start time of the laminar flow formation event. On the date of the event (5 November 2020) laminar flow formed first on Mount Sumbing at 00 UTC. This laminar flow only lasted one hour. Then the Ri value shows the presence of laminar flow on Mount Sindoro at 01 UTC. This situation lasted for three hours in the morning (Table II).

Laminar flow also occurred at 15 UTC on Mount Sumbing for one hour which was then followed by a reappearance at 18 UTC. This condition was also continued at the appearance of laminar flow at 22 UTC on Mount Sindoro.

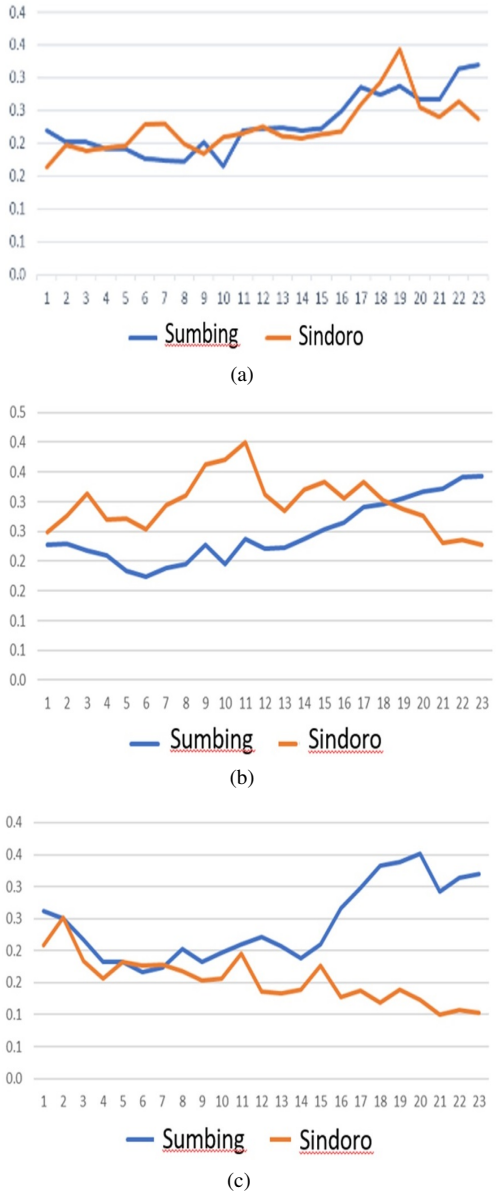

FIG. 12: Time series graph of Froude Number at Mount Arjuno (blue) and Mount Welirang (orange) in the 700 mb layer (a) 4 November (b) 5 November dan (c) 6 November.

On 4 and 6 November 2020 the formation of laminar flow also occurred several times on the four mountains, overall laminar flow conditions are more dominant on Mount Arjuno and Mount Sindoro. This can be seen from the distribution of $Ri > 1$ values that occur more in these two locations.

C. Mountain Waves

Based on the calculation of the Froude Number on Mount Arjuno and Welirang (Fig. 9), the value of Fr on both moun-

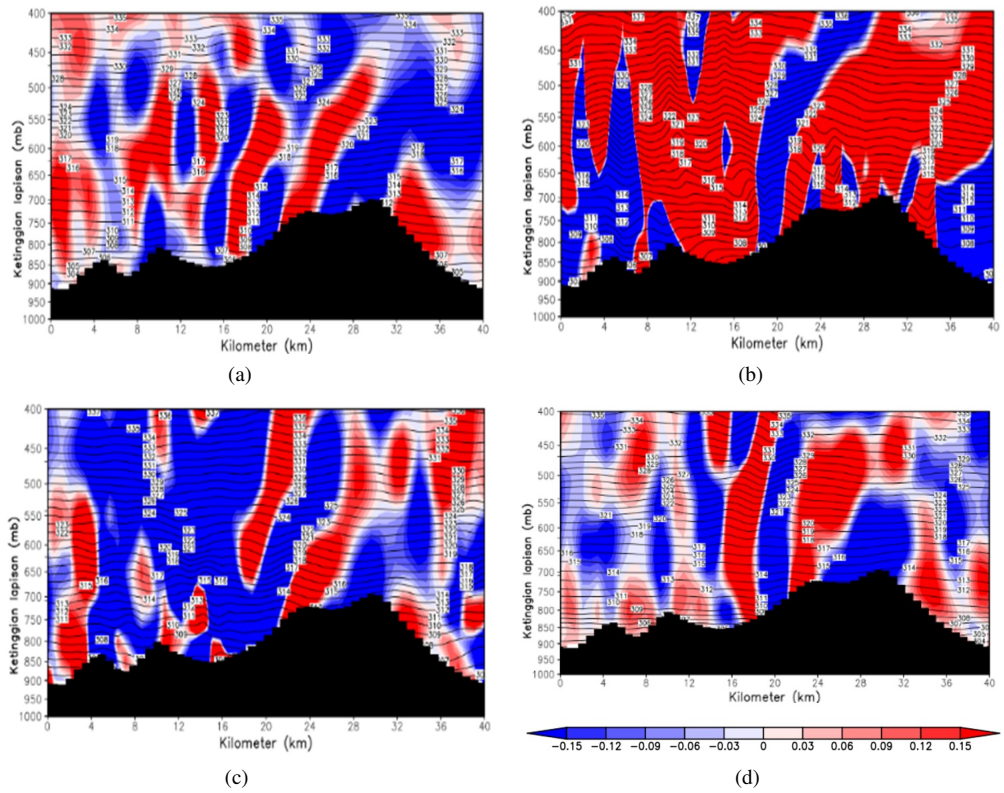

FIG. 13: Vertical velocity (m/s) and isentropic contours at Mount Sumbing (a) 5 November 01 UTC (b) 5 November 08 UTC (c) 5 November 09 UTC (d) 5 November 15 UTC.

tains only ranges from 1 $s^{(}-2)$ to 0.4 $s^{(}-2)$. The Froude Number pattern shows an increase on the 4th (before the event) and then a decrease on the 6th (after the event).

Based on the visualisation of vertical velocity and isentropic contours, mountain waves on Mount Arjuno began to form on 4 November. The mountain wave appeared at 22 UTC, characterised by an increase in vertical velocity (Fig. 10). This phenomenon then weakened on 5 November at 02 UTC. However, the mountain wave strengthened again until it reached its maximum vertical velocity at 08 UTC. Then the wave started to disappear on the 5th at 16 UTC.

In the area of Mount Welirang, there is a difference in the timing of the beginning of the formation of mountain waves. The formation of mountain waves occurred first on Mount Welirang and then followed by events on Mount Arjuno. The wave started to appear on the 4th at 16 UTC (Fig. 11). The wave weakened at 18 UTC, but then strengthened again until it reached the maximum vertical velocity on the 5th at 01 UTC. Then the wave started to dissipate at 14 UTC.

The model outputs of vertical velocity parameters and isentropic contours have linear results with dynamic stability conditions. Based on these two parameters, the appearance of mountain waves can be seen on Mount Welirang first on 4 November at 16 UTC, which is then followed by the appearance on Mount Arjuno on 4 November at 18 UTC.

In the Central Java region, on 4 November, the Fr values at both locations showed the same pattern, namely an increase until the early morning of 5 November. However, during the event (5 November) in the afternoon there was a different pattern between the two mountains. Fr values tended to decrease on Mount Sindoro and increase on Mount Sumbing. This condition persisted until 6 November (Fig. 12).

Based on the picture of vertical velocity and isentropic contours, a mountain wave formed on Mount Sumbing on 5 November at 01 UTC (Fig.13). This mountain wave continued to persist constantly and reached maximum strength at 08 UTC. This peak vertical velocity condition lasted for one hour until 09 UTC. The phenomenon then weakened at 15 UTC. Overall, there was a constant wave pattern, high wind speed and tight isentropic contours.

Similar conditions also occurred in the Mount Sindoro region. A mountain wave formed at the same time, on 4 November at 21 UTC. This mountain wave continued to persist constantly and reached its peak on 5 November at 07 UTC. This peak condition of vertical velocity strengthening also lasted for two hours until 09 UTC. This wave was weakened at 10 UTC (Fig. 14).

The image of vertical velocity and isentropic contours have linear results with the calculation of Richardson Number (dynamic stability). Based on these two parameters, the appearance of mountain waves can be seen since early morning on 5 November. However, there is a slight time difference between laminar flow conditions and wave formation.

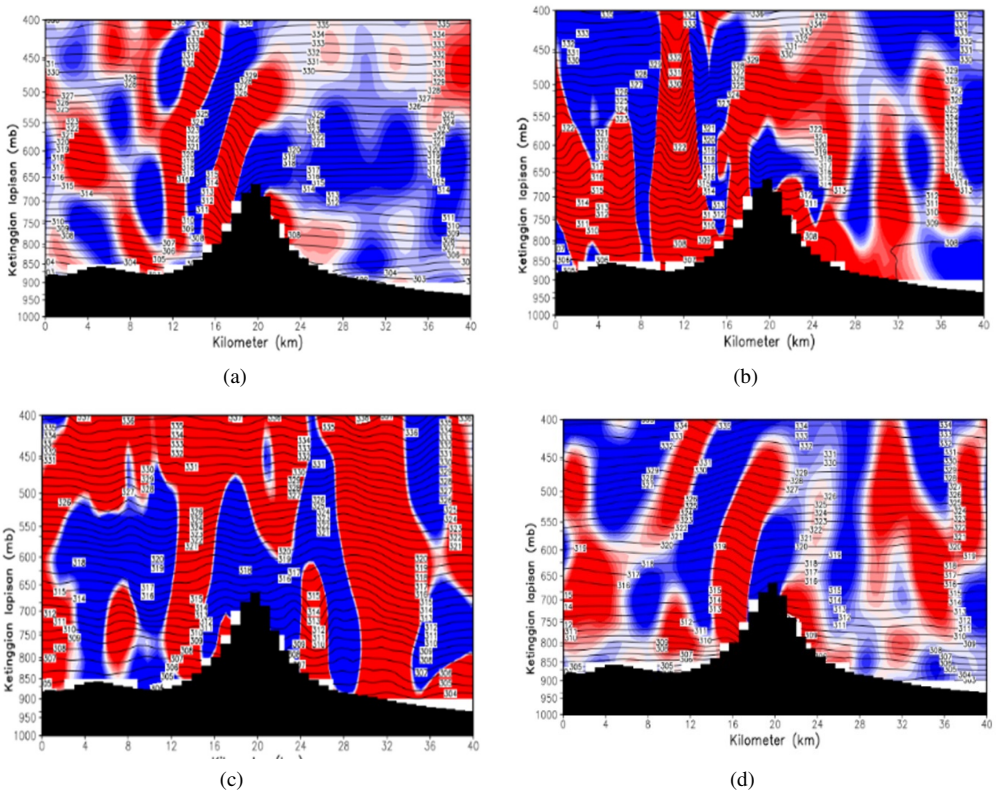

FIG. 14: Vertical velocity (m/s) and isentropic contours at Mount Sindoro (a) 4 November 21 UTC (b) 5 November 07 UTC (c) 5 November 09 UTC (d) 5 November 10 UTC.

IV. CONCLUSION

Based on the results of the research, it can be concluded that the mountain waves that occur on the four mountains are influenced by the Australian Monsoon. This is indicated by the occurrence of mountain waves that occurred first in East Java and followed by the Central Java region. The mountain waves that occur in the four locations are formed when the Froude Number value is below 1. The parameters used (static stability, Ricardson Number, and vertical velocity) can describe the mountain wave events well. In the future, further research is needed with different time periods and locations to obtain the characteristics of each mountain wave parameter in the Indonesian region, especially the Java Island region.

[1] J.R. Holton, and G. J. Hakim, "An introduction to dynamic meteorology", Fifth 597 edition, Academic Press, 2012. eBook ISBN: 9780123848673
[2] B.H.K. Tjasyono, dan S.W.B. Harijono, "Meteorologi Indonesia Volume I", Cetakan ke IV, BMKG. Jakarta. 2012,
[3] C.D. Ahrens, "Meteorology today: an introduction to weather, climate, and the environment", Cengage Learning Canada Inc, 2015.
[4] J-H. Qian, A.W. Robertson, and V. Moron, "Interactions among ENSO, the monsoon, and diurnal cycle in rainfall variability over Java, Indonesia", Journal of the Atmospheric Sciences, 2010, 67.11: 3509-3524.
[5] B. Wang, I-S. Kang, and J-Y Lee, "Ensemble simulations of AsianAustralian monsoon variability by 11 AGCMs", Journal of Climate, 2004, 17.4: 803-818.
[6] NOAA, 2004, "LAMINAR FLOW", https://w1.weather.gov/glossary/ index.php?word=LAMINAR. Agustus 2023.
[7] COMET, 2007, "Mountain Wave and Downslope Winds", http://www.meted.ucar.edu/mesoprim/mtnwave/. Agustus 2023.
[8] D.R. Durran, and B.K. Joseph, "The effects of moisture on trapped mountain lee waves", Journal of the Atmospheric Sciences, vol. 39, no. 11, p. 2490-2506, 1982.
[9] J.H. Holton, "An introduction to dynamic meteorology", American Journal of Physics, vol. 41, no. 5, p. 752-754, 2004.
[10] R.B. Stull, "Practical meteorology: an algebra-based survey of atmospheric science", University of British Columbia, 2015.
[11] P.A. Reinecke, and R.D. Dale, "Estimating topographic blocking using a Froude number when the static stability is nonuniform", Journal of the Atmospheric Sciences, vol. 65, no. 3, p. 1035-1048, 2008.
[12] J. Maruhashi, P. Serro, and M. Belo-Pereira, "Analysis of mountain wave effects on a hard landing incident in Pico aerodrome using the AROME model and airborne observations", Atmosphere vol. 10, no.7, p. 350, 2019.
[13] A. Kristianto, F.D. Claudia, and R.H.Virgianto, "Identification

of Mountain Waves and Their Characteristics in the Central Java Region based on the WRF Numerical Weather Model", Trends in Sciences, vol. 20, no. 10, p. 5827-5827, 2023.

[14] GNfI, "Fenomena Awan Topi yang Kompak Muncul pada 7 Gunung di Jawa", https://www.goodnewsfromindonesia.id/2020/11/10/fenomena-awan-topi-yang kompak-muncul-pada-7-gunung-di-jawa. Oktober 2022.

[15] BMKG, 2020, "Analisis Dinamika Atmosfer Dasarian I November 2020", https://www.bmkg.go.id/berita/?p=analisis-dinamika-atmosfer-dasarian-i november2020 & lang =ID&tag=dinamika-atmosfer, November 2022.

[16] W.C. Skamarock, *et al.*, "A description of the advanced research WRF version 4", NCAR tech. note ncar/tn-556+ str 145 .2019.

[17] Kinter III, James L. "The Grid Analysis and Display System (GrADS)", NASA NTRS, vol. 1, no. 26, p. 189387, 1994. https://ntrs.nasa.gov/citations/19950011076

[18] M. Niazkar, and S.H. Afzali, "Application of Excel spreadsheet in engineering education", First International and Fourth National Conference on Engineering Education, Shiraz University, 2015.